Spine

SPINE Volume 47, Number 10, pp 764–772

BASIC SCIENCE

Electrical Stimulation-Mediated Tissue Healing in Porcine Intervertebral Disc Under Mechanically Dynamic Organ Culture Conditions

Mohamad Kanan, BS,[a] Oliver Eby, BS,[b] Amey Kelkar, PhD,[b] Hassan Serhan, PhD,[b,c] Yehuda Zodak, PhD,[c] Sulaiman Aldoohan, PhD,[d] Haitham Elsamaloty, PhD,[d] Vijay Goel, PhD,[a,e] and Eda Yildirim-Ayan, PhD[a]

Study Design. Porcine intervertebral discs (IVDs) were excised and then drilled to simulate degeneration before being electrically stimulated for 21 days while undergoing mechanical loading. The discs were then analyzed for gene expression and morphology to assess regeneration.

Objective. The purpose of this study was to investigate the effectiveness of the electrical stimulation of IVD treatment as an early intervention method in halting the progression of degenerative disc disease using an ex-vivo porcine model.

Summary of Background Data. Treatments for degenerative disc disease are limited in their efficacy and tend to treat the symptoms of the disease rather than repairing the degenerated disc itself. There is a dire need for an early intervention treatment that not only halts the progression of the disease but contributes to reviving the degenerated disc.

Methods. Lumbar IVDs were extracted from a mature pig within 1 hour of death and were drilled with a 1.5 mm bit to simulate degenerative disc disease. Four IVDs at a time were then cultured in a dynamic bioreactor system under mechanical loading for 21 days, two with and two without the electrical stimulation treatment. The IVDs were assessed using histological analysis, magnetic resonance imaging, and quantitative reverse transcriptase polymerase chain reaction to quantify the effectiveness of the treatment on the degenerated discs.

Results. IVDs with electrical stimulation treatment exhibited extensive annular regeneration and prevented herniation of the nucleus pulposus (NP). In contrast, the untreated group of IVDs were unable to maintain tissue integrity and exhibited NP herniation through multiple layers of the annulus fibrosus. Gene expression showed an increase of extracellular matrix markers and antiinflammatory cytokine interleukin-4 (IL-4), while decreasing in pro-inflammatory markers and pain markers in electrically stimulated IVDs when compared to the untreated group.

Conclusion. The direct electrical stimulation application in NP of damaged IVDs can be a viable option to regenerate damaged NP and annulus fibrosus tissues.

Key words: bioreactor, degenerative disc disease, electrical stimulation, intervertebral disc, mechanical loading, organ culture, pain reduction, tissue regeneration.

Spine 2022;47:764-772

Lower back pain affects approximately one-third of the United States population and accrues costs of over $90 billion annually.[1–3] While the mechanisms are not entirely known, it is well known that one of the primary causes of back pain is damaged or degenerated intervertebral discs (IVDs).[4] Between two cartilaginous endplates, the IVD is composed of shock-absorbing gelatinous nucleus pulposus (NP) and tough collagen-rich annulus fibrosus (AF), which encircles the NP. Inflammation, aging, and/or excessive mechanical loading, damage the AF structure often resulting in NP herniation, degeneration, and increased pain. While the pain due to disc degeneration is certainly complex and may have many sources, studies demonstrate that in early-stage degeneration, the pain is associated with increased pro-inflammatory gene expression.[5–7] Hence, many studies use inflammatory markers as a metric for degeneration and/or pain given that they are two concomitant events.

The IVD is an avascular tissue and the only avenue for nutrient supply is perfusion from the vertebral endplates adjacent to highly vascularized vertebral bone.[8] This perfusion is governed via the physiological loading experienced by IVDs as well as by the osmotic gradient sustained by the

From the [a]Department of Biomedical Science, College of Medicine and Life Sciences, University of Toledo, Toledo, OH; [b]Department of Bioengineering, College of Engineering, University of Toledo, Toledo, OH; [c]Rainbow Medical Innovation, Herzyliya Pituachi, Israel; [d]Department of Radiology, College of Medicine and Life Sciences, University of Toledo, Toledo, OH; and [e]Department of Orthopaedic Surgery, University of Toledo Medical Center, Toledo, OH.

Acknowledgment date: May 14, 2021. First revision date: December 14, 2021. Acceptance date: January 5, 2022.

Mohamad Kanan and Oliver Eby contributed equally.

This research was funded in part by National Science Foundation, the Center for Disruptive Musculoskeletal Innovations.

Address correspondence and reprint requests to Eda Yildirim-Ayan, PhD, Nitschke Hall 1610 N. Westwood Toledo, OH 43606; E-mail: eda.yildirimayan@utoledo.edu

DOI: 10.1097/BRS.0000000000004331

negatively charged glycosaminoglycans that are ubiquitous in the NP.[9,10] The osmotic gradient pulls water and nutrients into the NP after the outflow of fluid caused by each vertebral motion.[10,11] As such, the electric potential in the IVD, can be viewed as a landmark for IVD health—or lack thereof—with disc damage showing marked decreases in electrical potentials and osmotic gradient.[12,13] In damaged IVDs, nutrition flow is interrupted which leads to degenerative disc disease.[14] Poillot *et al*[15] showed that mechanical loading of an IVD is inherently connected to the electrical potential in the NP and AF tissues.

In fact, the electrical stimulation of damaged tissue has been utilized as a therapeutic technique for tissue regeneration for decades.[16] Miller *et al*[17] extracted human NP and AF cells and cultured them in IL-1α in order to simulate an inflammatory environment before applying a pulsed electromagnetic field (PEMF) to the in vitro cultures. The pulsed electromagnetic field was able to partially reduce the expression of inflammatory markers IL-1α, MMP13, and IL-6. In a similar study, Shin *et al*[18] isolated human AF cells and cultured them with inflammation-induced macrophages. This coculture was then stimulated with 150 mV for 48 hours. Ultimately, the electro-stimulation was able to reduce the expression of inflammatory markers but antiinflammatory markers were not assessed. There have been various other studies both in vitro[19] and in vivo[20] that assess the effects of electric stimulation on lower back pain. However, to the knowledge of the authors at this time, the in vivo studies do not assess the expression of both pro- and antiinflammatory markers, nor do they insert the electrode directly into the NP, opting instead to study the effects of interstitial electric stimulation. There is, however strong support for applying electric stimulation directly to piezoelectric tissues, such as the IVD, for the purpose of tissue regeneration and pain reduction.[15,21]

In this study, a proprietary DisCure treatment was used to apply electrical stimulation to damaged discs to promote tissue regeneration. Our aim was to investigate the effect of electrostimulation directly on ex vivo NP tissue. Our hypothesis was that recreating the electro-osmotic gradient within the tissue would promote tissue regeneration and reduce pro-inflammatory and pain markers. To test our hypothesis, electrical stimulation was applied to the damaged IVDs under organ culture conditions for three weeks. Untreated damaged IVDs were used as a control. The structural, morphological, and molecular changes in IVD upon electrical stimulation treatment were assessed. The successful completion the study provided valuable data prior to comprehensive animal studies to understand the role of direct electrical stimulation on tissue regeneration and immunomodulation in in vivo.

MATERIALS AND METHODS

IVD Isolation

Lumbar IVDs were harvested from skeletally mature female pigs. IVDs were isolated, cleared of debris, and distributed between control and experimental groups to eliminate the potential effects of different levels. Each sample consisted of a 3 mm vertebral bony part, an intact endplate, and the IVD. Following the isolation, IVDs were washed with EtOH and soaked in phosphate buffered saline, 3% penicillin/streptomycin, 1.5% fungizone for 15 minutes.

IVD Defect Creation and Electrode Implantation

Within an hour after isolation, defects were created in each IVD to mimic the most common disc herniation location. A 1.5 mm drill bit was used to drill the IVDs based on established degeneration protocols.[22,23] IVD drilling was monitored using an X-ray system to confirm nucleolus pulposus penetration without damaging the endplates. Following the degeneration induction, the DisCure electrode was inserted from the posterior lateral side of each disc contralateral to the drilling site. Supplemental Figure 1, http://links.lww.com/BRS/B852, illustrates the major steps followed in IVD preparation for the study. The electrode was inserted into the NP and its position was verified using the same X-ray system. The electrodes were then connected to the DisCure pulse generator device providing 1.1 V with a duty cycle of 96%. Grounding wires were also connected to the DisCure device and placed in the media surrounding each IVD. The DisCure device is a control box that can be programmed to emit various electrical pulses for any specified length of time that are delivered via the lead wires that were injected into the IVDs. The stimulation waveform was in rectangular shape with 0.003 Hz frequency. Then, the IVDs were moved to the EQUicycler Organ Culture Platform for applying the mechanical loading conditions.

Ex Vivo Organ Culture

Since the IVD is avascular and relies heavily on its electro-osmotic gradient as well as the mechanical loading of natural movement, it is crucial when performing tissue culturing to simulate the mechanical loading regimen of normal in vivo motion.[22,24,25] The EQUicycler Organ Culture Platform was utilized to apply cyclic loading to the IVDs for 21 days within the incubator (37C, 5% CO_2). The EQUicycler mechanism and design are based on a well-established bioreactor system created by the research team for IVD tissue regeneration applications.[24,26] The EQUicycler consists of four major components: (1) a two-phase high torque stepper motor mechanism, (2) a PEEK moving plate hosting IVDs, (3) a fixed plate, (4) and a controller. The EQUicycler applies mechanical strain to the IVDs through cyclic vertical displacement in the moving plate against the IVDs. Figure 1 demonstrates the components of the computer-controlled organ culture bioreactor and electrical stimulation platform.

Two samples were treated with electrical stimulation, while the other two were controls in each experiment. The organ culture chambers were filled with Dulbecco Modified Eagle Medium supplemented with 10% FBS, 1% penicillin/streptomycin, 0.5 μg/mL fungizone, and 1:500 Primocin. In addition, 1.5% of 5 M NaCl with 0.4 M KCl was added to the cell culture media to prevent swelling. 50% of the

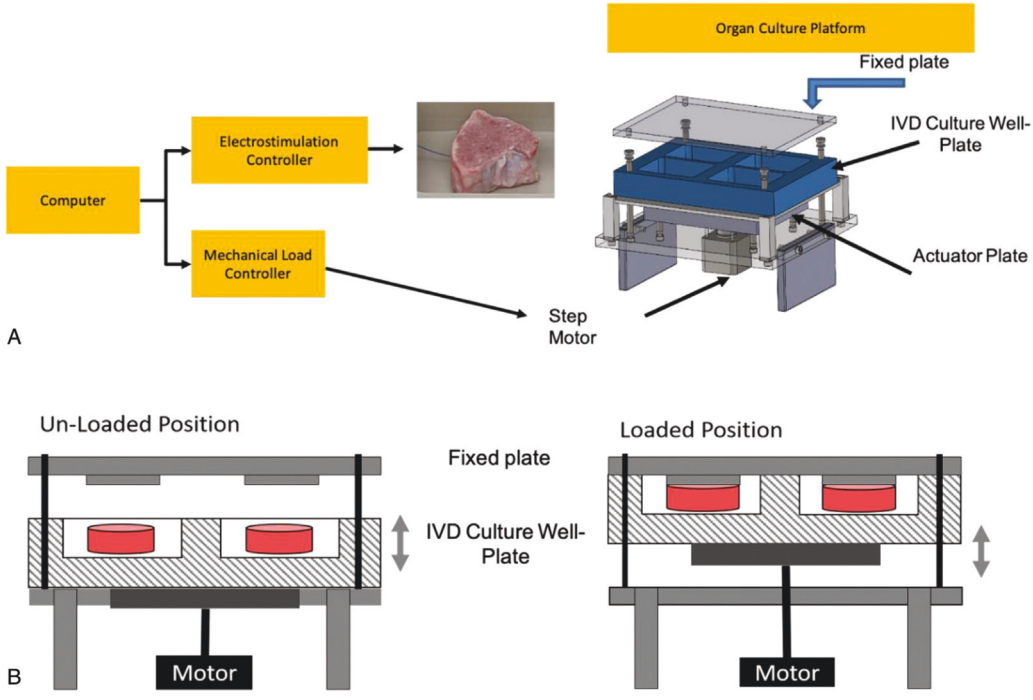

Figure 1. (**A**) The main components of computer-controlled dynamic organ culture bioreactor and electrical stimulation platform. (**B**) The schematic representation of organ culture platform in loaded and unloaded positions to exert the biphasic loading regimen. IVD indicates intervertebral disc.

medium was refreshed every 3 days. The whole EQUicycler was then placed in the incubator to conduct organ culture for 21 days. The 0.2 MPa constant pressure was applied to the IVDs to mimic the constant pressure exerted on the IVDs by torso weight, muscles, and tendons for twenty hours per day. For four hours each day, a cyclic equiaxial loading regimen creating 0.6 MPa pressure with 0.1 Hz frequency was applied to the IVDs to simulate the average pressure in lumbar spine[27,28] and to simulate the average loading frequency encountered in lumbar region during diurnal period.[29–31]

Structural and Morphological Characterization

MRI Analysis

MR images were acquired to observe the morphological changes of the IVDs following 21 days of organ culture. T2 weighted images slices of 3 mm in thickness were acquired using Fast Spin-Echo pulse sequence imaging protocols. Using spinal coil, the samples were oriented in the coronal plane in a spinal configuration with the cranial side facing the spinal coil. Imaging was obtained in the sagittal, coronal, and transverse planes for each sample.

Histological Analysis

The IVDs used for MR image analysis were subsequently placed in 10% normalized formalin for histological characterization. IVDs were then dissected and processed on a Sakura Tissue TEK VIP 5 processor. Following this, the samples were immersed in paraffin and embedded into a tissue cassette before being cut on a LEICA RM 2235 microtome in 5 μm sections and placed on slides. The slides were then stained with H&E.

Biological Characterization

Gene Expression Analysis

Gene expression analysis was done via quantitative reverse transcriptase polymerase chain reaction of inflammatory markers (TNF-α, COX2, IL-12), antiinflammatory markers (IL-4 and IL-10), pain markers (BDKRB1, COMT, NGF, CGRP), matrix enzymes (MMP-3, MMP-13), and phenotypic markers (Aggrecan, SOX-9). Briefly, AF and NP tissues were collected and minced into small pieces, then RNA was extracted using TRIzol reagent, reverse transcription was performed using the Omniscript RT kit per the manufacturer's instructions. Quantitative reverse transcriptase polymerase chain reaction was performed using SYBR Green master mix. GAPDH was used as the normalizing gene. Primer sequences were obtained from published literature as listed in Table 1 [32–41] and purchased from Integrated DNA Technologies. Data were analyzed using the Ċ ΔΔCt method.

Statistical Analysis

Statistical analysis was conducted through Minitab using Student *t* test and one-way ANOVA. All values are reported as the mean ± the standard deviation. Sample sizes were determined by power analysis using one-way ANOVA, an alpha level of 0.05, power of 0.8, and effect size of 1.20.

TABLE 1. Forward and reverse primers for real-time PCR

Gene	Forward Primer (5′–3′)	Reverse Primer (5′–3′)	Ref
MMP-3	TCCTGATGTTGGTTACTTCAGCAC	TTGACAATCCTGTAAGTGAGGTCATT	[36]
MMP-13	CATGAGTTTGGCCATTCCTT	GTGGCTTTTGCCAGTGTAGG	[36]
COX-2	GGCTGCGGGAACATAATAGA	AAAAGCAGCTCTGGGTCA AA	[37]
IL-12	CACTCCTGCTGCTTCACAAA	CGTCCGGAGTAATTCTTTGC	[38]
TNF-α	ATGAGCACTGAGAGCATGATCCG	CCTCGAAGTGCAGTAGGCAGA	[39]
IL-10	GCCTTCGGCCCAGTGAA	AGAGACCCGGTCAGCAACAA	[40]
IL-4	GCGAGAAAGAACTCGTGCATGG	CTCAGGAGGCTCTTCATGCAC	[39]
Aggrecan	CAGGTGAAGACTTTGTGGACATC	GTGAGTAGCGGGAGGAGCCC	[36]
SOX-9	CGGTTCGAGCAAGAATAAGC	GTAATCCGGGTGGTCCTTCT	[41]
NGF	GGCCCAATAACGGCTTTTCC	TTTAGTCCAGTGGGCTTGGG	[42]
BDKRB1	TCCTGGTCCAGGTGAGAGTGA	GGTTCAGGCAGCTGTTGCCA	[43]
COMT	CTGGACACCATCGACACCTA	CAGCCGAGTAGCCACAGTAA	[44]
CGRP	TGCCCAGAAGAGAGCCT	TGAAGGTCCCTGCGGC	[45]
GAPDH	GTTTGTGATGGGCGTGAACC	AGCTTGACGAAGTGGTCGTT	[36]

Each organ culture study of four samples was repeated twice for a total of eight. Four IVDs were assigned as a treatment group (n = 4) and another four were assigned as control group (n = 4) without electrical stimulation. Pain and inflammatory markers were analyzed after sectioning each NP into eleven samples and each AF into seven samples.

RESULTS

IVD Defect Creation and Electrode Implantation

X-ray fluoroscopy was used to confirm the IVD damage creation using drilling without penetrating the endplate. The position of the inserted titanium electrode was also confirmed with X-ray fluoroscopy. The X-ray images of the drill bit position and electrode within the IVDs is given in Supplemental Figure 2, http://links.lww.com/BRS/B852.

Gross Morphological Observations

Immediately upon completion of the 21-day organ culture, the IVDs were dissected to observe the morphological differences between the treatment and control groups. Figure 2 demonstrates the gross observations from the dissected control and treated IVDs. The data showed significant morphological differences in the integrity of the NP as well as the AF between the treated and untreated IVDs. The AF for the treatment group showed healthy recovery from the

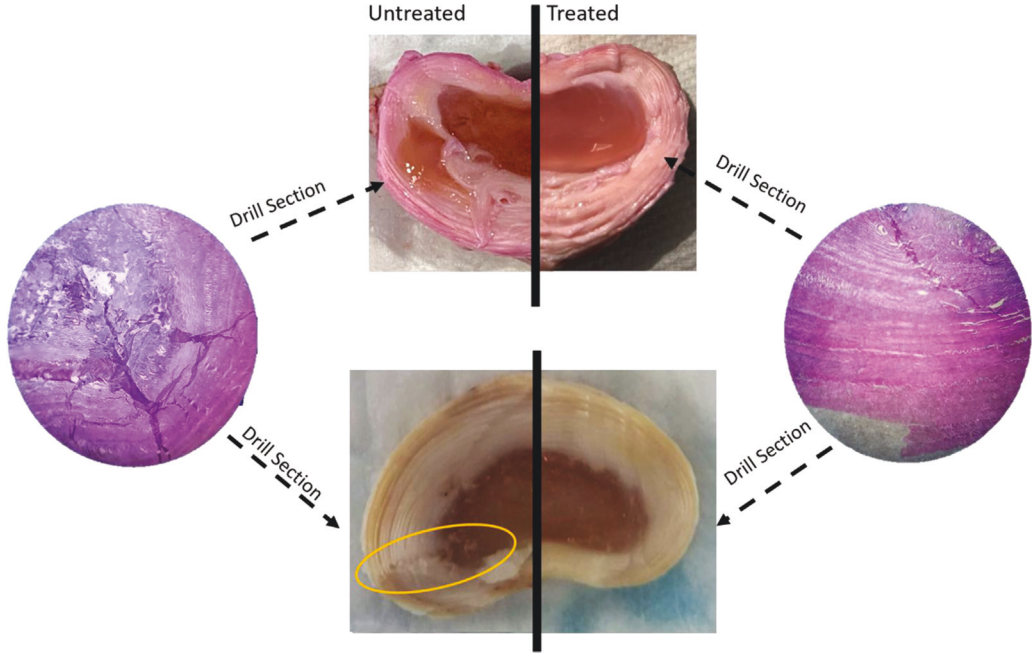

Figure 2. (**A**) The optical gross images of untreated and treated IVDs following 21-days of organ culture. (**B**) The histological images of drill site for untreated IVDs stained with H&E (4 ×). (**C**) The optical images of untreated and treated IVDs at the drill site. (**D**) The histological images of drill site for treated IVDs stained with H&E (4 ×). IVD indicates intervertebral disc.

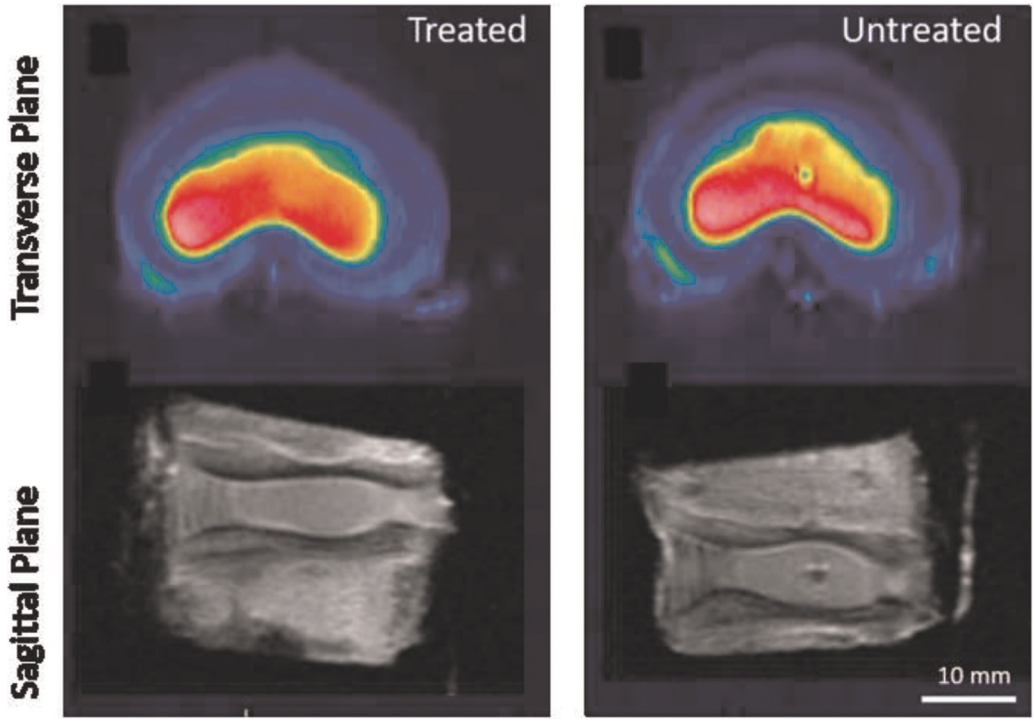

Figure 3. MR images obtained postexperiment. (**A**) Transverse plane image of treated IVD. (**B**) Sagittal plane image of treated IVD. (**C**) Transverse plane image of untreated IVD. (**D**) Sagittal plane image of untreated IVD. IVD indicates intervertebral disc.

drilling and prevented any herniation of the NP through the layers of the AF. This is in direct contrast to the nonstimulated samples in the control group where the NP pushed through the defect in the AF causing herniation and further deteriorated IVD integrity.

Histology Analysis

Figure 2 also shows sectioned views in the transverse plane of both treated and untreated IVDs following H&E staining. The expanded areas of the control group showed visible damage to the NP-AF border at the drill site while the treatment group shows significantly better healing around its drill site. The untreated IVD clearly shows the remnants of the drilled section through the AF while the stimulated IVD shows no lasting marks from the drilling or the electrode insertion and so demonstrates significant regrowth of the AF tissue.

MRI Analysis

Radiologic imaging displayed a stark difference between the treated and untreated IVDs following the organ culture period. Figure 3 shows the transverse and sagittal plane magnetic resonance imaging (MRI) data of treated and untreated IVDs. The treated IVDs displayed a distinct and continuous border between the NP and AF. Additionally, the treated IVDs demonstrated a healed defect site with no herniations. In contrast, the untreated IVDs displayed herniations at the defect site with the NP protruding past the proximal layers of the AF. The dot observed in the center of untreated NP suggested that ECM regeneration was not completed for the untreated group and the defect was still visible even after 21 days of organ culture.

Gene Expression Analysis

To understand the effect of electrical stimulation on IVDs at the molecular level, a comprehensive gene expression analysis was conducted on AF and NP sections of treated and untreated IVDs in all replicated experiments. The gene expression analysis of extracellular matrix-degrading enzymes MMP-3 and MMP-13 (Figure 4) demonstrated that the expression of both decreased significantly for the AF region of the disc upon electrical stimulation ($P < 0.05$). While there was no statistical difference of MMP-3 expression in the NP region, there was a statistically significant ($P < 0.005$) drop in MMP-13 expression in the NP within the treated group. The gene expression analysis of TNF-α and COX-2 revealed that, for the AF region, both decreased significantly ($P < 0.05$ and $P < 0.005$, respectively) compared to untreated IVDs (Figure 4). For the NP region, TNF-alpha expression was not changed upon electrical stimulation although COX-2 expression decreased dramatically ($P < 0.005$) upon treatment. The expressions of pain markers, BDKRB1, COMT, and CGRP, in the NP and AF sections were assessed in the treated and untreated IVDs (Figure 4). There was a statistically significant downregulation in pain markers in both AF and NP sections in treated IVDs compared to counterparts in untreated IVDs. The one exception being the expression of COMT as there was no statistical difference in COMT expression in the AF section between treated and untreated IVDs. Figure 4 also

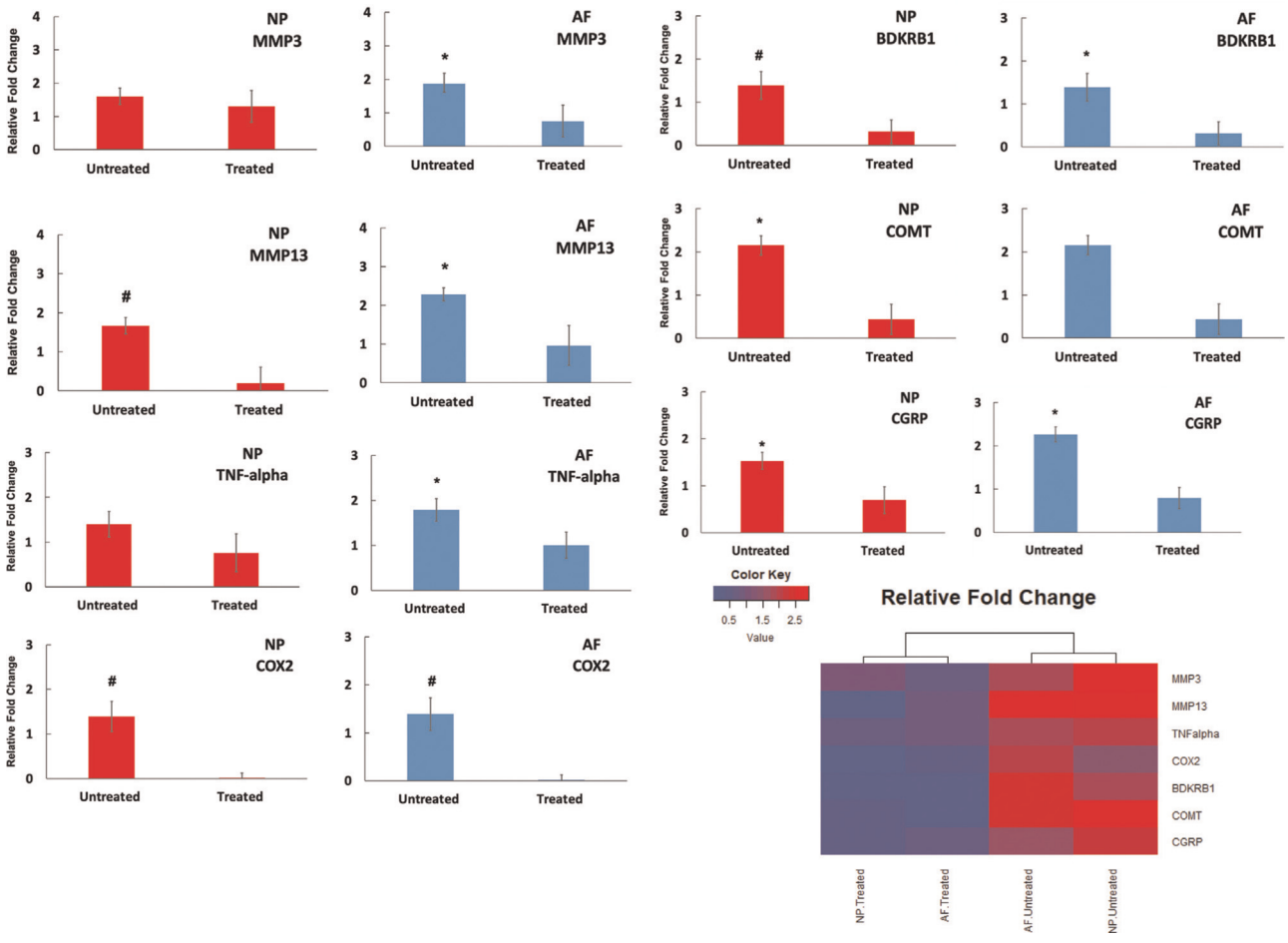

Figure 4. The relative fold changes of extracellular matrix breakdown genes of MMP3 and MMP13, pro-inflammatory cytokines of TNF-alpha and COX-2, pain markers of BDKRB1, COMT, and CGRP in AF and NP sections of untreated (control) and electrical stimulation treated IVDs. All data were expressed as the mean standard deviation. Differences between groups were analyzed using the Student *t* test, with $P < 0.05$ (indicated as *) and $P < 0.005$ (indicated as #). AF indicates annulus fibrosus; IVD, intervertebral disc; NP, nucleus pulposus.

summarizes the relative fold change values associated with catabolic genes in a heatmap format to demonstrate the differences between the treated and untreated IVDs clearly. In this case, the pro-inflammatory markers and pain markers are not desirable for regeneration and so lower expressions of these genes is shown in blue, while the red signifies higher expression levels.

To understand the degree of potential IVD regeneration, the gene expression of ACAN and SOX-9 were analyzed. There was a significant ($P < 0.005$) ACAN upregulation in the treated NP and AF sections with fold changes of 13.23 ± 0.39 and 8.04 ± 0.47, respectively. Gene expression data revealed that electrical stimulation significantly ($P < 0.005$) increased SOX-9 expression by 4.04 ± 0.4 fold in NP and 10.24 ± 0.16 fold in AF compared to untreated IVDs. In addition, for antiinflammatory markers, IL-4 demonstrated elevated gene expressions ($P < 0.005$) in treated IVDs compared to untreated counterparts both in AF and NP sections. However, there were no statistically significant changes in expressions of IL-10 between treated and untreated IVDs either in AF or in NP sections. Figure 5 demonstrates the relative fold changes in anabolic genes associated with tissue regeneration and summarizes those values in a heatmap format. As demonstrated with Figures 4 and 5, the DisCure electrical stimulation increased the expression of antiinflammatory markers while promoting the IVD extracellular matrix regeneration and reducing the expressions of pro-inflammatory markers.

DISCUSSION

In this study, we analyzed the effects of electrical stimulation on IVDs, showing increased ECM regeneration while reducing the pro-inflammatory and pain markers. The comprehensive morphological and molecular analyses were conducted to understand the effectiveness of electrical stimulation in IVD tissue healing and pain management.

The MRI results (Figure 3) displayed a clear difference between treated and untreated groups. The most prominent differences were observed in disc morphology, NP and AF boundaries, and extent of degeneration at the defect site. Annular defects increase the risk of disc herniation and the protrusion of the NP[42] so it was necessary that the induced defect mimic natural defects by puncturing through the annular rings, compromising their ability to contain the

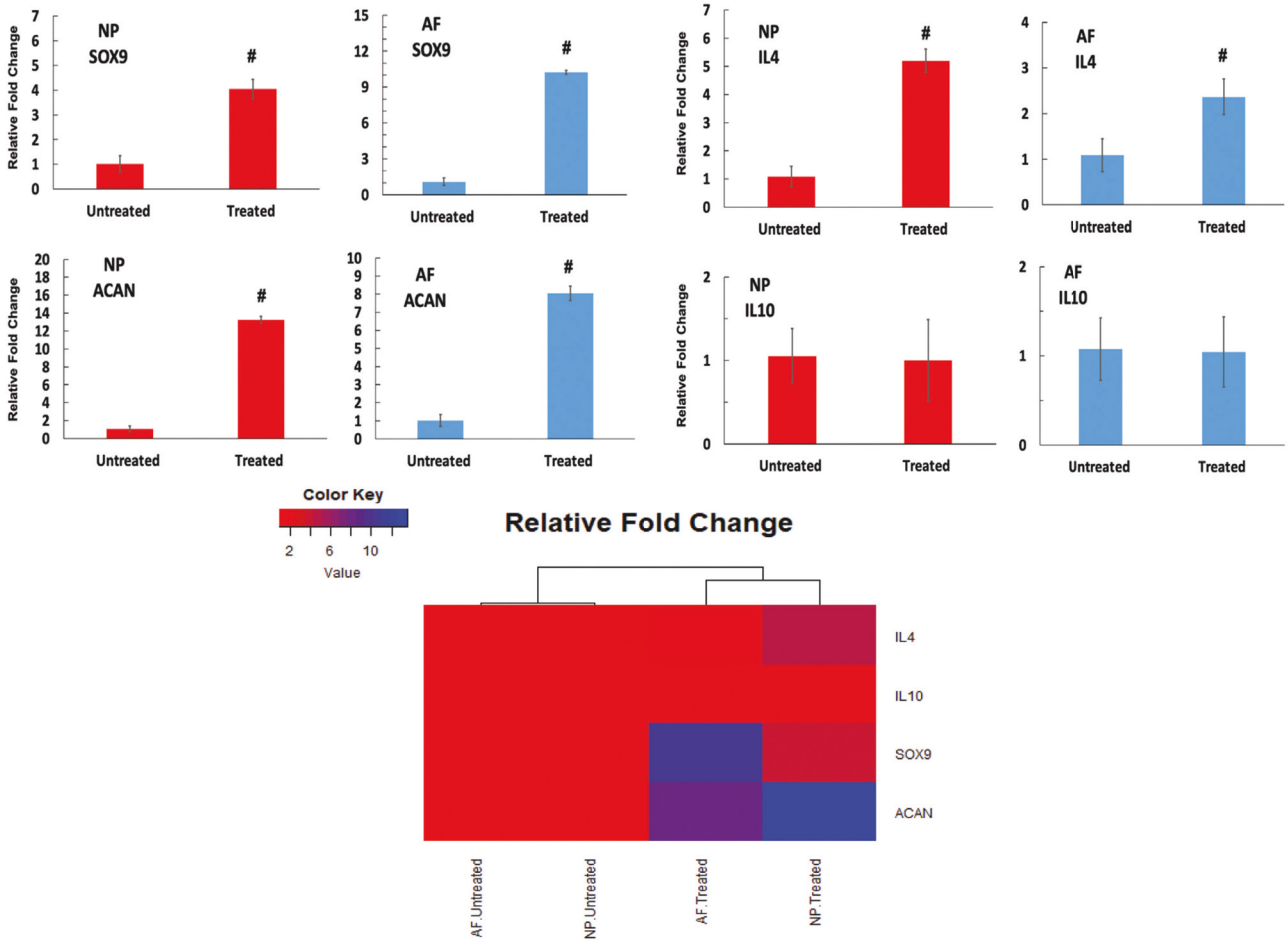

Figure 5. The relative fold changes of antiinflammatory cytokines of IL-4 and IL-10 along with the IVD ECM regeneration markers of SOX9 and ACAN in AF and NP sections of untreated (control) and electrical stimulation treated IVDs. All data were expressed as the mean standard deviation. Differences between groups were analyzed using the Student *t* test, with $P < 0.05$ (indicated as –) and $P < 0.005$ (indicated as #). AF indicates annulus fibrosus; IVD, intervertebral disc; NP, nucleus pulposus.

NP. Factoring in the mechanical stress, which greatly increases the risk of herniation,[43] the IVDs were expected to herniate under the mechanical loading. Observing the defect site was therefore critical in determining the healing potential of the treatment. The defect was almost invisible in the treated group while the untreated group displayed a significant loss of the normal border between the NP and AF with herniations at the defect site (Figure 2). The treated discs, on the other hand, did not herniate but maintained the NP within its boundaries. These results are supported by the histological analysis as the drill and electrode sites from the untreated group clearly demonstrate the loss of tissue integrity with little to no regeneration while images of the treated group show significant collagen fiber reattachment and healing in both the drill and electrode insertion sites.

Gene expression analysis revealed the underlying mechanisms for the tissue regeneration in the treatment group (Figures 4 and 5). Under normal physiological conditions, MMP-3 and MMP-13 are involved in IVD homeostasis as they regulate ECM production and provide defensive mechanisms against tumorigenesis.[44] However, upon tissue damage, these enzymes can be over-activated by pro-inflammatory cytokines including TNF-alpha and COX-2.[45] The heatmap in Figures 4 and 5 comprehensively shows the trend that electrical stimulation of IVDs was able to not only curb the expression of MMP-3 and MMP-13, but also decrease the expression of pro-inflammatory cytokines TNF-alpha, and COX-2 while increasing the expression of antiinflammatory cytokine IL-4 expression.

Concomitantly, we expected to have down-regulated pain markers as a result. The expression of BDKRB1, COMT, and CGRP was significantly down-regulated in the treatment group when compared with the controls suggesting that reducing inflammation while promoting tissue regeneration also reduces pain (Figure 4).

We further analyzed the expression of extracellular matrix related genes including SOX-9 and ACAN. The reason to focus on ACAN is that it is a chondroitin sulfate proteoglycan, which is abundantly present in healthy IVDs.[46] It provides high osmotic swelling pressure to compensate for the compressive loads on the spine.[47] The ACAN expression increased significantly in AF and NP sections of

the treated IVDs compared to counterparts in untreated IVDs (Figure 5). Its upregulation is, therefore, an indication of restored IVD health and ECM regeneration. The reason for tracking SOX-9 gene expression is that the transactivation of ACAN is primarily regulated by SOX-9. SOX-9 expression was upregulated in the NP and AF regions, which means that it further triggered the expression of ACAN which subsequently helped ECM regeneration as confirmed in MRI/histology analysis.

The aforementioned results can be attributed to the charged NP. Charging the NP of the disc enhances the negatively charged proteoglycans and the disc's natural pumping function. Poillot *et al*[15] showed that the mechanical loading of an IVD is inherently connected to the electrical potential in the NP and AF tissues. Thus, a healthy IVD during normal motion is supplied with electric potentials that may work in conjunction to support the intake of nutrients through membranes as well as affect the stiffness of the tissue.[48] By providing electric stimulation as well as the diurnal mechanical loading regimen, this study re-enforced the electric potential that is normal to a healthy IVD. As Ning *et al*[49] reports, this can have a vast variety of effects on the macro and microenvironmental scale within tissues.

Overall, this study revealed that electrical stimulation of IVDs shows great promise as an early intervention therapy for damaged disc regeneration. The electrical stimulation increased the matrix regeneration while reducing inflammation and pain markers. Taken together, our organ culture porcine model demonstrated that IVD hemostasis can be restored in damaged IVDs through electrical stimulation treatment. However, further studies need to be conducted to optimize the electrical pulse waveforms, electrical stimulation period as well as to examine the physiological mechanisms and responsible pathways behind observed tissue regeneration upon electrical stimulation treatment.

➢Key Points

- ❑ Organ culture bioreactor with dynamic mechanical loading was utilized to culture damaged ex-vivo porcine disc with and without electrical stimulation for 21 days.
- ❑ The electrical stimulation repaired the damaged disc demonstrated by the upregulation of extracellular matrix gene expressions (SOX9 and Aggrecan) and morphological changes in the damaged areas using histology and MR imaging.
- ❑ The pain markers with the damaged disk were downregulated upon electrical stimulation for 21 days.
- ❑ The electrical stimulation downregulated the pro-inflammatory markers including TNF-a and COX-2 while increased the antiinflammatory associated genes IL-4 and IL-10 for AF and NP sections of the disc.

Supplemental digital content is available for this article. Direct URL citations appearing in the printed text are provided in the HTML and PDF version of this article on the journal's Web site (www.spinejournal.com).

References

1. Dagenais S, Caro J, Haldeman S. A systematic review of low back pain cost of illness studies in the United States and internationally. *Spine J* 2008;8:8–20.
2. Freburger JK, Holmes GM, Agans RP, et al. The rising prevalence of chronic low back pain. *Arch Intern Med* 2009;169:251–8.
3. Johannes CB, Le TK, Zhou X, Johnston JA, Dworkin RH. The prevalence of chronic pain in United States adults: results of an Internet-based survey. *J Pain* 2010;11:1230–9.
4. Iordanova E, Røe C, Keller A, et al. Long-lasting low back pain and MRI changes in the intervertebral discs. *Tidsskr Nor Laegeforen* 2010;130:2260–3.
5. van den Berg R, Jongbloed EM, de Schepper EIT, Bierma-Zeinstra SMA, Koes BW, Luijsterburg PAJ. The association between pro-inflammatory biomarkers and nonspecific low back pain: a systematic review. *Spine J* 2018;18:2140–51.
6. Boisson M, Borderie D, Henrotin Y, et al. Serum biomarkers in people with chronic low back pain and Modic 1 changes: a case-control study. *Sci Rep* 2019;9:10005.
7. da Cruz Fernandes IM, Pinto RZ, Ferreira P, Lira FS. Low back pain, obesity, and inflammatory markers: exercise as potential treatment. *J Exerc Rehabil* 2018;14:168–74.
8. Urban JPG, Smith S, Fairbank JCT. Nutrition of the intervertebral disc. *Spine* 2004;29:2700–9.
9. Mohd Isa IL, Abbah SA, Kilcoyne M, et al. Implantation of hyaluronic acid hydrogel prevents the pain phenotype in a rat model of intervertebral disc injury. *Sci Adv* 2018;4:eaaq0597.
10. Bergknut N, Smolders LA, Grinwis GC, et al. Intervertebral disc degeneration in the dog. Part 1: anatomy and physiology of the intervertebral disc and characteristics of intervertebral disc degeneration. *Vet J* 2013;195:282–91.
11. Adams MA, McMillan DW, Green TP, Dolan P. Sustained loading generates stress concentrations in lumbar intervertebral discs. *Spine (Phila Pa 1976)* 1996;21:434–8.
12. Werbner B, Spack K, O'Connell GD. Bovine annulus fibrosus hydration affects rate-dependent failure mechanics in tension. *J Biomech* 2019;89:34–9.
13. Zhu Q, Gao X, Chen S, Gu W, Brown MD. Effect of intervertebral disc degeneration on mechanical and electric signals at the interface between disc and vertebra. *J Biomech* 2020;104:109756.
14. Roughley PJ. Biology of intervertebral disc aging and degeneration: involvement of the extracellular matrix. *Spine (Phila Pa 1976)* 2004;29:2691–9.
15. Poillot P, O'Donnell J, O'Connor DT, et al. Piezoelectricity in the intervertebral disc. *J Biomech* 2020;102:109622.
16. Holzbauer M, Rigler R. Electric shock and the regeneration of the corneal epithelium of rabbits. *Nature* 1951;168:919.
17. Miller SL, Coughlin DG, Waldorff EI, Ryaby JT, Lotz JC. Pulsed electromagnetic field (PEMF) treatment reduces expression of genes associated with disc degeneration in human intervertebral disc cells. *Spine J* 2016;16:770–6.
18. Shin J, Hwang M, Back S, et al. Electrical impulse effects on degenerative human annulus fibrosus model to reduce disc pain using micro-electrical impulse-on-a-chip. *Sci Rep* 2019;9:5827.
19. Wang Z, Hutton WC, Yoon ST. The effect of capacitively coupled (CC) electrical stimulation on human disc nucleus pulposus cells and the relationship between CC and BMP-7. *Eur Spine J* 2017;26:240–7.
20. Gerasimov AA, Meshchaninov VN, Shcherbakov DL. Mechanisms of pathogenetic treatment with interstitial electrostimulation for spinal pain syndrome. *Vopr Kurortol Fizioter Lech Fiz Kult* 2019;96:12–8.
21. Hayes AJ, Melrose J. Electro-stimulation, a promising therapeutic treatment modality for tissue repair: emerging roles of sulfated glycosaminoglycans as electro-regulatory mediators of intrinsic repair processes. *Adv Ther* 2020;3:.

22. Daly C, Ghosh P, Jenkin G, Oehme D, Goldschlager T. A review of animal models of intervertebral disc degeneration: pathophysiology, regeneration, and translation to the clinic. *Biomed Res Int* 2016;2016:5952165.
23. Lim KZ, Daly CD, Ghosh P, et al. Ovine lumbar intervertebral disc degeneration model utilizing a lateral retroperitoneal drill bit injury. *J Vis Exp* 2017;55753.
24. Elsaadany M, Winters K, Adams S, Stasuk A, Ayan H, Yildirim-Ayan E. Equiaxial strain modulates adipose-derived stem cell differentiation within 3D biphasic scaffolds towards annulus fibrosus. *Sci Rep* 2017;7:12868.
25. Gantenbein B, Illien-Jünger S, Chan CW, et al. Organ culture bioreactors–platforms to study human intervertebral disc degeneration and regenerative therapy. *Curr Stem Cell Res Ther* 2015;10:339–52.
26. Elsaadany M, Harris M, Yildirim-Ayan E. Design and validation of equiaxial mechanical strain platform, EQUicycler, for 3D tissue engineered constructs. *Biomed Res Int* 2017;2017:3609703.
27. Chan SC, Ferguson SJ, Gantenbein-Ritter B. The effects of dynamic loading on the intervertebral disc. *Eur Spine J* 2011;20:1796–812.
28. Jamison Dt. Cannella M, Pierce EC, Marcolongo MS. A comparison of the human lumbar intervertebral disc mechanical response to normal and impact loading conditions. *J Biomech Eng* 2013;135:91009.
29. Long RG, Zderic I, Gueorguiev B, et al. Effects of level, loading rate, injury and repair on biomechanical response of ovine cervical intervertebral discs. *Ann Biomed Eng* 2018;46:1911–20.
30. Lu D, Solomonow M, Zhou B, Baratta RV, Li L. Frequencydependent changes in neuromuscular responses to cyclic lumbar flexion. *J Biomech* 2004;37:845–55.
31. Costi JJ, Stokes IA, Gardner-Morse MG, latridis JC. Frequency-dependent behavior of the intervertebral disc in response to each of six degree of freedom dynamic loading: solid phase and fluid phase contributions. *Spine (Phila Pa 1976)* 2008;33:1731–8.
32. Bracci-Laudiero L, Aloe L, Caroleo MC, et al. Endogenous NGF regulates CGRP expression in human monocytes, and affects HLA-DR and CD86 expression and IL-10 production. *Blood* 2005;106: 3507–14.
33. Gao H, Zhang Q, Chen J, et al. Porcine IL-6, IL-1, and TNF-regulate the expression of pro-inflammatory-related genes and tissue factor in human umbilical vein endothelial cells. *Xenotransplantation* 2018;25:e12408.
34. Gonzalez LM, Williamson I, Piedrahita JA, Blikslager AT, Magness ST. Cell lineage identification and stem cell culture in a porcine model for the study of intestinal epithelial regeneration. *PLoS One* 2013;8:e66465.
35. Ignjacev-Lazich I, Kintsurashvili E, Johns C, et al. Angiotensin-converting enzyme regulates bradykinin receptor gene expression. *Am J Physiol Heart Circ Physiol* 2005;289:H1814–20.
36. Jaworski LM, Kleinhans KL, Jackson AR. Effects of oxygen concentration and culture time on porcine nucleus pulposus cell metabolism: an in vitro study. *Front Bioeng Biotechnol* 2019;7:64.
37. Kommareddy M, McAllister R, Ganjam V, Turk JR, Laughlin MH. Upregulation of cyclooxygenase-2 expression in porcine macula densa with chronic nitric oxide synthase inhibition. *Vet Pathol* 2011;48:1125–33.
38. Ryan M, O'Shea C, Collins C, O'Doherty JV, Sweeney T. Effects of dietary supplementation with Laminaria hyperborea, Laminaria digitata, and Saccharomyces cerevisiae on the IL-17 pathway in the porcine colon. *J Anim Sci* 2012;90:263–5.
39. Shi J, Zhou X, Wang Z, Kurra S, Niu J, Yang H. Increased lactic acid content associated with extracellular matrix depletion in a porcine disc degeneration induced by superficial annular lesion. *BMC Musculoskelet Disord* 2019;20:1–9.
40. Terenina E, Sautron V, Ydier C, et al. Time course study of the response to LPS targeting the pig immune gene networks. *BMC Genomics* 2017;18:1–14.
41. Vandenbroucke V, Croubels S, Martel A, et al. The mycotoxin deoxynivalenol potentiates intestinal inflammation by Salmonella typhimurium in porcine ileal loops. *PLoS One* 2011;6:e23871.
42. McGirt MJ, Eustacchio S, Varga P, et al. A prospective cohort study of close interval computed tomography and magnetic resonance imaging after primary lumbar discectomy: factors associated with recurrent disc herniation and disc height loss. *Spine* 2009;34: 2044–51.
43. Rannou F, Corvol M, Revel M, Poiraudeau S. Disk degeneration and disk herniation: the contribution of mechanical stress. *Joint Bone Spine* 2001;68:543–6.
44. McCawley LJ, Crawford HC, King LE, Mudgett J, Matrisian LM. A protective role for matrix metalloproteinase-3 in squamous cell carcinoma. *Cancer Res* 2004;64:6965–72.
45. Kelley MJ, Rose AY, Song K, et al. Synergism of TNF and IL-1 in the induction of matrix metalloproteinase-3 in trabecular meshwork. *Invest Ophthalmol Vis Sci* 2007;48:2634–43.
46. Roughley PJ, Melching LI, Heathfield TF, Pearce RH, Mort JS. The structure and degradation of aggrecan in human intervertebral disc. *Eur Spine J* 2006;15:S326–32.
47. Takimoto A, Kokubu C, Watanabe H, et al. Differential transactivation of the upstream aggrecan enhancer regulated by PAX1/9 depends on SOX9-driven transactivation. *Sci Rep* 2019;9:4605.
48. Ahn AC, Grodzinsky AJ. Relevance of collagen piezoelectricity to "Wolff's Law": a critical review. *Med Eng Phys* 2009;31: 733–41.
49. Ning T, Zhang K, Heng BC, Ge Z. Diverse effects of pulsed electrical stimulation on cells - with a focus on chondrocytes and cartilage regeneration. *Eur Cell Mater* 2019;38:79–93.